Investigation on Pole-Slot Combinations for Permanent-Magnet Machines with Concentrated Windings

F. Libert, J. Soulard

Department of Electrical Machines and Power Electronics, Royal Institute of Technology
100 44 Stockholm, Sweden, phone: +46 87907757, fax: +468205268,
e-mail: florence@ekc.kth.se

Abstract - The aim of this paper is to find the best concentrated windings layouts for high pole number permanent-magnet (PM) machines. Pole and slot numbers are varied from 4 to 80 and 6 to 90 respectively. Among all the pole/slot combinations, those giving the highest winding factors are provided. Harmonics in the magneto-motive force (MMF), torque ripple and radial magnetic forces that cause vibration are analysed in order to sort out the best layouts.

Keywords – Permanent magnet machines, concentrated windings, high pole number.

I. INTRODUCTION

Using permanent magnet (PM) machines with a high pole number for low speed direct-drive applications has recently gained great interest [1]. By getting rid of the gearbox, a PM direct drive can indeed provide better performance and/or be lighter than the induction motor with a gearbox. For these machines, concentrated windings around the teeth, with their simple structure and short end-windings, are very attractive [2].

In [3] and [4], it is showed how to find concentrated winding layouts giving high winding factors for up to 18 poles. In this paper, the focus is on PM machines with higher pole numbers. It is possible to find high winding factors by varying the slot pitch as studied in [2] or alternatively by finding a good combination between slot and pole numbers. This second approach is more challenging because of the high number of possible combinations when the pole number is high. It is investigated in this study.

The aim of this paper is to sort out the different winding layouts and possible slot/pole combinations in order to simplify the choice of a layout. With this regard, the winding factors of the investigated concentrated windings, the MMF-harmonics, the torque ripple and the radial magnetic forces are calculated and analyzed for some interesting combinations.

II. WINDING LAYOUTS AND WINDING FACTORS

A. Determination of the winding layout for a two-layer winding

Double-layer windings are investigated since they have better properties such as shorter end-windings and more sinusoidal back-emf waveforms than one-layer windings [3], [5]. For different slot and pole combinations, the winding layout, i.e. the placement of the conductors of each phase in the slots, is determined. The method presented in [4] describes how to obtain the layout that gives the highest winding factor for given pole number p and slot number Q_s. The method is based on the decomposition of the number of slots per pole per phase q. It is similar to the method used for the large synchronous machines with a fractional value of q [6]. The method is described in figure 1 using Q_s = 24 and p = 26 as an example.

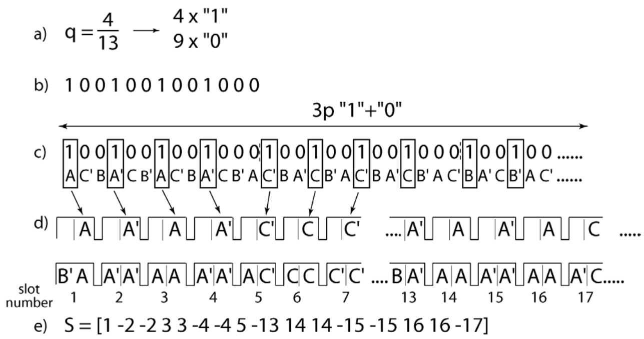

Figure 1. Winding layout determination for Q_s = 24, p = 26.

a) q is written as a fraction which is cancelled down to its lower terms: q=b/c =4/13 where b and c are integers.
b) A sequence of b-c = 9 zeros and b=4 ones is found, the "1" being distributed in the sequence as regularly as possible.
c) The sequence is repeated 3p/c =Q_s/b =6 times, and compared to the layout of the distributed winding with 3p slots and q = 1.
d) Conductors from the distributed winding corresponding to the "1" are kept and form one layer of the concentrated winding. The second layer is obtained by writing for each already obtained conductor, its corresponding return conductor on the other side of the tooth, i.e. A' for A, B' for B…
e) A vector S is written to describe the layout of one phase. It will be used to calculate the winding factor. The slots are numbered from 1 to Q_s. The vector consists of the numbers corresponding to the slots containing phase A. If the two layers of one slot contains phase A, then the number of the slot is written two times in the vector (see fig 1.e). For the conductors A', a minus is added to the corresponding slot numbers.

B. Method used to calculate the winding factor

The winding factor is calculated using the electromotive force (EMF) phasors [3]. The EMF phasor $\vec{E}_i$ of conductor *i* is:

$$\vec{E}_i = e^{j\frac{\pi . p}{Q_s} S(i)} \qquad (1)$$

The winding factor k_w for the fundamental can then be calculated using (2):

$$k_w = \frac{\left| \sum_{i=1}^{2Q_s/3} \vec{E}_i \right|}{n_l Q_s / 3} \qquad (2)$$

S is the sequence of conductors of 1 phase defined previously and n_l the number of layers.

For the example with $Q_s = 24$, $p = 26$, the sum of the EMF phasors is:

$$\sum_1^{16} \vec{E}_i = e^{j\frac{\pi p}{Q_s}} + 2e^{-2j\frac{\pi p}{Q_s}} + 2e^{3j\frac{\pi p}{Q_s}} + 2e^{-4j\frac{\pi p}{Q_s}} + e^{5j\frac{\pi p}{Q_s}}$$
$$+ e^{-13j\frac{\pi p}{Q_s}} + 2e^{14j\frac{\pi p}{Q_s}} + 2e^{-15j\frac{\pi p}{Q_s}} + 2e^{16j\frac{\pi p}{Q_s}} + e^{-17j\frac{\pi p}{Q_s}}$$

This gives a winding factor of 0.95.

C. *Winding factor calculations*

Winding factors for machines from 4 to 80 poles and 6 to 90 slots are calculated. This represents 935 pole/slot combinations. Table I shows the winding factors calculated for two-layer concentrated windings with p between 20 and 80, and Q_s between 15 and 90, with Q_s being divisible by 3. The method to find the winding layout with the highest winding factors presented above does not have to be applied for every combination. Indeed winding factors of some combinations can be found directly:

- Some combinations do not give a balanced winding. Those are the combination with the denominator c (q=b/c) that is multiple of the number of phases. There are represented in black in table I.
- Combinations with the same value of q have the same winding factor. The winding layout has the same basic sequence reproduced a certain number of times to get the required number of slots (see table II)
- For each Q_s, i.e. each line of the table, there is a periodicity of $2Q_s$: the winding layout and factors of combinations with Q_s slots and $p+2k.Q_s$ poles (k=0,1,2…) are the same. This is easily shown with (2) and (3):

  $\forall$ i integer, as S(i) is an integer

$$e^{j\frac{\pi p}{Q_s} S(i)} = e^{j\frac{\pi p}{Q_s} S(i)} e^{j2\pi S(i)} = e^{j\frac{\pi (p+2Q_s)}{Q_s} S(i)} \qquad (3)$$

- For each Q_s, i.e. each line of the table, there is a symmetry around the lines $p = k.Q_s$ where $k = 1,2,3\ldots$ Combinations with $p = Q_s$-k and $p = Q_s$ +k, with k=1,2,3… have the same layout and winding factor. This is shown below:

$$\left| \sum_i e^{j\frac{\pi p}{Q_s} S(i)} \right| = \left| \sum_i \cos\frac{\pi p}{Q_s} S(i) + j \sum_i \sin\frac{\pi p}{Q_s} S(i) \right|$$

$$= \left[\left(\sum_i \cos\frac{\pi p}{Q_s} S(i) \right)^2 + \left(\sum_i \sin\frac{\pi p}{Q_s} S(i) \right)^2 \right]^{1/2}$$

For $p=Q_s$-k, the sum of cosinus and sinus terms can be rewritten as:

$$\sum_i \cos\frac{\pi (Q_s - k)}{Q_s} S(i) = \sum_i (\cos \pi S(i) \cos\frac{\pi k S(i)}{Q_s} + \underbrace{\sin \pi i \sin\frac{\pi k S(i)}{Q_s}}_{=0})$$

$$= \sum_i \cos\frac{\pi (Q_s + k)}{Q_s} S(i)$$

$$\sum_i \sin\frac{\pi (Q_s - k)}{Q_s} S(i) = \sum_i (\underbrace{\sin \pi S(i) \cos\frac{\pi k S(i)}{Q_s}}_{=0} - \sin\frac{\pi k S(i)}{Q_s} \cos \pi i)$$

$$= -\sum_i \sin\frac{\pi (Q_s + k)}{Q_s} S(i)$$

This leads to :

$$\left| \sum_i e^{j\frac{\pi (Q_s - k)}{Q_s} S(i)} \right| = \left| \sum_i e^{j\frac{\pi (Q_s + k)}{Q_s} S(i)} \right|$$, which

means that the winding factors for $p = Q_s$-k and $p = Q_s + k$, with k=1,2,3 are equal.

- It has been noticed that the winding factor increases and decreases as shown in figure 2. Figure 2 shows also the symmetries and periodicity described previously. It can be concluded that only some combinations with p slightly lower than Q_s should be further investigated. The other cases giving high winding factors will be deduced from these calculations.

Table II also shows that winding factors up to 0.954 can be reached. In the following, the windings presenting high winding factors i.e. with Q_s around p will be investigated further.

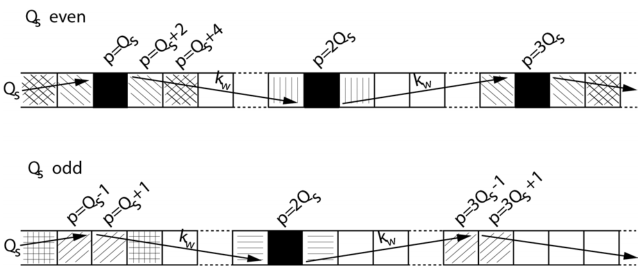

Figure 2. Evolution of the winding factor k_w for a slot number Q_s and different pole numbers p.

(Boxes filled with the same pattern have the same winding factor and layout. Black boxes are combinations where concentrated windings are not possible.)

TABLE I Winding factors for different combinations of pole numbers p and slot numbers Qs

Qs\p	4	6	8	10	12	14	16	18	20	22	24	26	28	30	32	34	36	38	40	42
6	0.866		0.866	0.500		0.500	0.866		0.866	0.500		0.500	0.866		0.866	0.500		0.500	0.866	
9	0.617	0.866			0.866	0.617	0.328		0.328	0.617	0.866			0.866	0.617	0.328		0.328	0.617	0.866
12	1		0.866				0.866		…	…		…	…		0.866				0.866	
15			0.621	0.866					0.866	0.621		…	…		…	…		0.621	0.866	
18		1	…	0.647	0.866						0.866	0.647	…	…	…	…		…	…	…
21			…	…		0.866	0.890		0.953	0.953		0.890	0.866		…	…		…	…	
24			1	…		0.760	0.866			0.950		0.950			0.866	0.760		…	…	
27				…	…	…	…	0.866	0.877	0.915		0.954	0.954		0.915	0.877	0.866	…	…	…
30				1		…	…		0.866	0.874		0.936				0.936		0.874	0.866	
33						…	…		…	0.866		0.903	0.928		0.954	0.954		0.928	0.903	
36					1	…	…		…	…	0.866	0.867				0.953		0.953		
39						…	…		…	…		0.866	0.863		0.918	0.936		0.954	0.954	
42						1	…		…	…		…	0.866		0.890	0.913		0.945	0.953	

Qs\p	42	44	46	48	50	52	54	56	58	60	62	64	66	68	70	72	74	76	78	80
45		0.955	0.955			0.927		0.886	0.859	0.866	…	…	…	…	…		…	…	…	…
48		0.950	0.954		0.954	0.950			0.905		0.857	0.866		…	…		…	…		…
51		0.933	0.944		0.955	0.955		0.944	0.933		0.901	0.880		0.866	…		…	…		…
54		0.915	0.930		0.949	0.954		0.954	0.949		0.930	0.915		0.877	0.854	0.866	…	…	…	…
57		0.932	0.912		0.937	0.946		0.955	0.955		0.946	0.937		0.912	0.932		0.852	0.866		…
60		0.874	0.892			0.936			0.954		0.954			0.936			0.892	0.874		0.866
63	0.866	0.850	0.871	0.890	0.905	0.919			0.948	0.953	0.955	0.955	0.953	0.948			0.919	0.905	0.890	0.871
66		0.866	0.849		0.887	0.903		0.928	0.938		0.951	0.954		0.954	0.951		0.938	0.928		0.903
69		…	0.866		0.867	0.884		0.914	0.925		0.943	0.949		0.955	0.955		0.949	0.943		0.925
72	…	…	…	0.866	0.847	0.867			0.911		0.933		0.950	0.953	0.954		0.954	0.953	0.950	
75		…	…		0.866	0.846		0.880	0.895		0.920	0.930		0.945			0.955	0.955		
78		…	…		…	0.866		0.863	0.879		0.906	0.918		0.936	0.943		0.952	0.954		0.954
81	…	…	…	…	…	…	0.866	0.845	0.860	0.877	0.890	0.904	0.915	0.925	0.933		0.946	0.951	0.954	0.955
84		…	…		…	…		0.866	0.845		0.876	0.890		0.913			0.939	0.945		0.953
87		…	…		…	…		…	0.866		0.859	0.874		0.899	0.910		0.929	0.936		0.947
90	…	…	…	…	…	…		…	…	0.866	0.843	0.859	0.874	0.886			0.918	0.927	0.936	

0.866	k_{w1}= 0.866, q=1/2, 1/4		k_{w1}= 0.945, q=3/8, 3/10	0.955	Qs=21+6k, p=Qs±1, k = 0, 1, 2 …
	k_{w1}= 0.902, q=3/7, 3/11		k_{w1}= 0.951, q=5/14, 5/16	0.954	Qs=24+6k, p=Qs±2, k = 0, 1, 2 …
	k_{w1}= 0.933, q=2/5, 2/7		not allowed	…	k_{w1} < 0.866

TABLE II Winding layout for some combinations of pole numbers p and slot numbers Qs
(A' designed the return conductor corresponding to conductor A, the colors refer also to table II)

Slot/pole combination or number of slot per pole per phase q	Winding layout
q = 2/5, 2/7	$\ldots\lvert C'A\lvert A'A'\lvert AB'\lvert BB\lvert B'C\lvert C'C'\lvert CA'\lvert AA\lvert A'B\lvert B'B'\lvert BC'\lvert CC\ldots$
q = 3/8, 3/10	$\ldots\lvert C'A\lvert A'A'\lvert AA\lvert A'B\lvert B'B'\lvert BB\lvert B'C\lvert C'C'\lvert CC\lvert\ldots$
q = 3/7, 3/11	$\ldots\lvert CA'\lvert AB'\lvert BB\lvert B'C'\lvert CA\lvert A'A'\lvert AB'\lvert BC'\lvert CC\lvert C'A\lvert A'B\lvert B'B'\lvert BC'\lvert CA'\lvert AA\lvert A'B\lvert B'C\lvert C'C'\ldots$
q = 5/14, 5/16	$\ldots\lvert C'A\lvert A'A'\lvert AA\lvert A'A'\lvert AA\lvert A'B\lvert B'B'\lvert BB\lvert B'B'\lvert BB\lvert B'C\lvert C'C'\lvert CC\lvert C'C'\lvert CC\ldots$
Qs = 12 + 6k, with k = 0, 1, 2 … p = Qs ± 2 If p/2 even If p/2 odd	$\ldots\underbrace{A\lvert A'A'\lvert A\ldots A\lvert A'A'\lvert A}_{Qs/6}\underbrace{B'\lvert BB\lvert B'\ldots B'\lvert BB\lvert B'}_{Qs/6}\underbrace{C\lvert C'C'\lvert C\ldots C\lvert C'C'\lvert C}_{Qs/6}\ldots$ $\underbrace{A\lvert A'A'\lvert A\ldots A'\lvert AA\lvert A'}_{Qs/6}\underbrace{B\lvert B'B'\lvert B\ldots B'\lvert BB\lvert B'}_{Qs/6}\underbrace{C\lvert C'C'\lvert C\ldots C'\lvert CC\lvert C'}_{Qs/6}\underbrace{A'\lvert\ldots\lvert A}_{Qs/6}\underbrace{B\lvert\ldots\lvert B'}_{Qs/6}\underbrace{C'\lvert\ldots\lvert C}_{Qs/6}$
Qs = 9 + 6k, with k = 0, 1, 2 … p = Qs ± 1	$\underbrace{A\lvert A'A'\lvert A\ldots A'\lvert AA\lvert A'}_{Qs/3}\underbrace{B\lvert B'B'\lvert B\ldots B'\lvert BB\lvert B'}_{Qs/3}\underbrace{C\lvert C'C'\lvert C\ldots C'\lvert CC\lvert C'}_{Qs/3}$

III. MMF AND HARMONICS

Analysing the MMF and its harmonics is of interest since it can cause extra iron losses in the rotor compared with distributed windings. The MMF is calculated analytically with the method fully described in [3]. The harmonics are calculated by taking into account the periodicity of the MMF waveform that is the number of symmetries in the winding. Independently of the number of poles, the period of the MM waveform is taken as the fundamental. The advantage is that the harmonic orders are integers. The harmonic interacting with the flux density from the permanent magnets and producing the average value of the torque is then the harmonic equal to the ratio between the number of poles and the number of periods in the MMF.

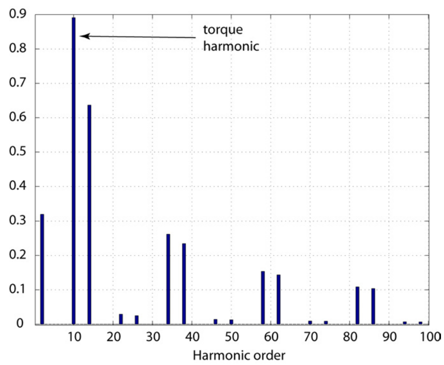

Figure 3. Harmonics in the MMF for double-layer concentrated windings, 48 slots and 40 poles (q=2/5)

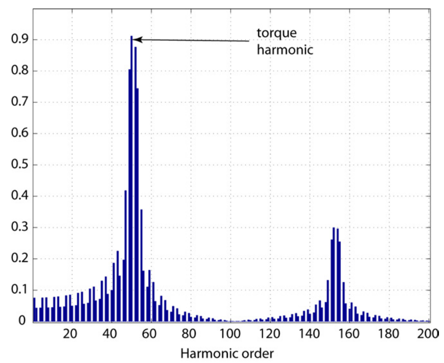

Figure 4. Harmonics in the MMF for double-layer concentrated windings, 51 slots and 50 poles

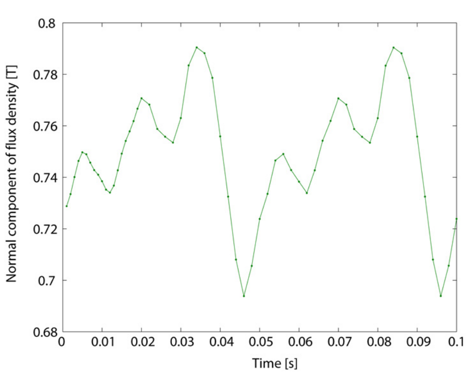

Figure 5. Time variation of the normal component of the total flux density, in the middle of the rotor iron between two permanent magnets, for a 72 slots, 64 poles motor

Figures 3 and 4 give the harmonics in the MMF for machines with double-layer concentrated windings and 48 slots, 40 poles (q=2/5) and 51 slots, 50 poles. The harmonics giving the torque are the 10th and the 50th for the 40 poles and 50 poles designs respectively. As can be seen on the figures, the MMFs contain many harmonics with high amplitude. The windings without symmetries also present many more harmonics in the MMF than those with symmetries (figure 3).

Due to these harmonics, alternating magnetic fields appear in the rotor. As can be seen on figure 5, the flux density in the rotor is indeed not constant. This gives rise to eddy currents in the permanent magnets and iron losses in the rotor iron. These losses should therefore be estimated during the design process when using concentrated windings. If they are too high, a laminated rotor and permanent magnets in small pieces can help.

IV. TORQUE RIPPLE

A. *Cogging torque*

Very low cogging torque can be achieved if the slot and pole numbers are chosen so that the least common multiple (LCM) between these numbers is large [3]. Windings with q=2/5 and q=3/8 have a lower LCM than the other windings and present a higher cogging torque (Table III). The closer the number of slots to the number of poles, the higher the LCM.

The combinations $p = Q_s-k$, $p = Q_s+k$ have the same winding factor, but the LCM is higher when $p = Q_s+k$ than the dual case $p = Q_s-k$.

Table III Lowest common multiple (LCM) and cogging torque of different surface mounted PM motors

p, Q_s, q	LCM	Cogging torque in % of rated torque
p=60, Q_s=72, q=2/5	360	1.4
p=64, Q_s=72, q=3/8	576	0.3
p=64, Q_s=60, q=5/14	960	0.03
p=64, Q_s=66, q=11/32	2112	0.003
p=62, Q_s=63, q=21/62	3906	0.003

B. *Torque ripple*

Finite element simulations are run to compute the torque for different winding layouts. An important aspect is to determine the initial position of the rotor in combination with the applied currents. The maximum torque is achieved for a surface mounted PM motor when the angle between the current vector and the PM flux vector is β=90 electrical degrees. Choosing that the current in phase A is equal to zero at the initial rotor position, means that the flux density should be at its maximum. A magnet should be aligned to the tooth or the slot that is the axis of symmetry of the phase A coils as shown on figure 6.

If the first A concentrated coil is around tooth 1, and the tooth are numbered as in figure 3, then the tooth that should be aligned to a magnet is given for different configurations in table IV. When the tooth number is not an integer it means that the magnet faces a slot.

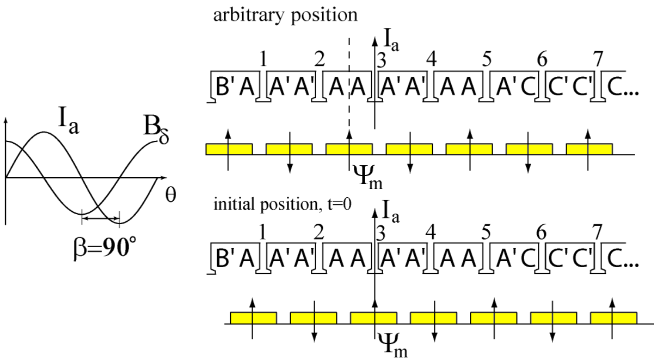

Figure 6. Initial position of a surface mounted PM motor. I_a is the current in phase A, B_δ is the airgap flux density

Table IV Initial rotor position

Q_s/p combination or value of q	Slot number
q=2/5	4.5
q=3/8	2
q=5/14	3
Qs = 12 + 6k, k = 0, 1, 2 … p = Qs ± 2, p even	$\frac{Q_s}{12}+\frac{1}{2}$
Qs = 12 + 6k, k = 0, 1, 2 … p = Qs ± 2, p odd	$\frac{Q_s}{3}+\frac{1}{2}$
Qs = 9 + 6k, k = 0, 1, 2 … p = Qs ± 1	$\frac{Q_s}{6}+\frac{1}{2}$

Surface mounted PM motors with different pole and slot numbers as those described in table IV were simulated at nominal load. The results give a torque ripple between 1 and 5% of the rated torque. It can be noticed that a design with high cogging torque can present lower torque ripple than a design with lower cogging torque as shown in tables III and V.

Table V Torque ripple of different surface mounted PM motors

p, Q_s, q	Torque ripple in % of rated torque
p=60, Q_s=72, q=2/5	2.6
p=64, Q_s=72, q=3/8	3.4
p=64, Q_s=60, q=5/14	3.2
p=64, Q_s=66, q=11/32	3.4
p=62, Q_s=63, q=21/62	4.4

Whatever the combination of slot and pole numbers, the PM machine with concentrated windings will present a much lower torque ripple than machine with distributed windings and one slot per pole and per phase without skewing. Those can have a torque ripple of 20% or more [7].

V. Magnetic Noise

Magnetic noise results from magnetic forces that make the stator vibrate. Radial forces are attractive forces between the stator and the rotor while tangential forces act on the rotor to produce torque. The forces that generate magnetic noise are mostly the radial forces [8]. FEM simulations are used to calculate the radial magnetic forces.

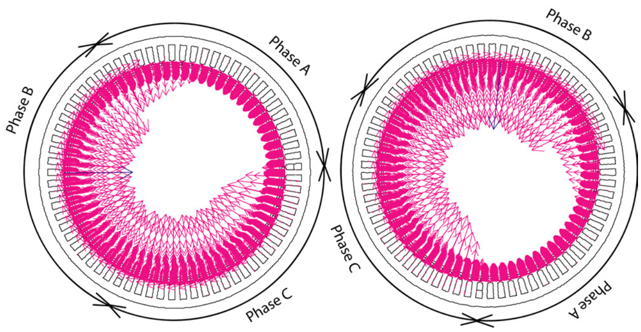

Figure 7. Radial magnetic forces on the stator of a 68 poles, 69 slots surface mounted PM motor, at different time

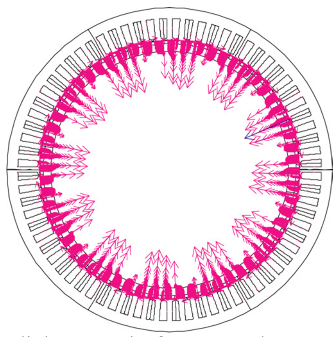

Figure 8. Radial magnetic forces on the stator of a 60 poles, 72 slots surface mounted PM motor

The computation relies on the Maxwell Stress method. For this computation, only the normal component of the flux density is taken into account (4).

$$\sigma(\theta,t)=\frac{1}{2\mu_0}B_n(\theta,t)^2 \qquad (4)$$

where σ is radial magnetic force density, θ the angular coordinate, t the time, μ_0 the permeability of free space and B_n the radial component of the airgap flux density.

The tangential component of the airgap flux density is neglected, since the iron material is many times more permeable than air. The flux lines indeed enter and leave the stator and rotor surfaces almost perpendicularly.

Figure 7 represents the radial magnetic force densities on the stator of a PM motor with 68 poles 69 slots at two different moments. It can be seen that the distribution of the magnetic forces on the stator is not symmetrical. The sum of these magnetic forces gives a resulting force that turns around with the time and generates noise and vibration in the machine. This resulting force is due to the asymmetry in the windings. The pole/slot combinations giving winding layouts without any symmetry such as combinations with Qs = 9+6k, k = 0,1,2…and p = Qs ± 1 are therefore not recommended. The magnetic pressure for a design with 60 poles, 72 slots and a symmetry in the winding in one sixth of the machine is represented on figure 8. It can be seen that, for this design, there is no resulting force as the forces are compensating each other.

VI. Conclusions

Some hints on how to choose layouts for PM machines with concentrated windings and high pole numbers are provided in this paper. First, the winding factors for different pole-slot combinations are calculated and some of the winding layouts giving high winding factor are described. By choosing one of these layouts, the performances of the design can be much improved.

However it should be taken into account that the concentrated windings cause alternating magnetic field in the rotor giving rise to rotor losses.

Depending on the pole and slot numbers combination, the cogging torque can be reduced. The torque ripple at load is harder to predict from the slot/pole combination, but it is always very low compared to a distributed winding machine without skewing and one slot per pole per phase.

Magnetic noise is also an issue for some PM machines with concentrated windings. The machines with winding layouts without any symmetry such as combinations with $Qs = 9+6k$, $k = 0,1,2\ldots$ and $p = Qs \pm 1$ have unbalanced radial forces that make the stator vibrates and produce noise.

Combinations of slot-pole numbers with high winding factors and windings with many periods in the layouts give the best performances and allow avoiding high magnetic noise.

VII. ACKNOWLEDGMENT

This work has been carried out within the Permanent Magnet Drive Program of the Competence Center in Electrical Engineering at the Royal Institute of Technology in Stockholm. Flux2D, software from Cedrat has been used for the finite element simulations.

VIII. REFERENCES

[1] Haring T., Forsman K., Huhtanen T., Zawadzki M., "Direct Drive – Opening a New Era in Many Applications", *Pulp and Paper Industry Technical Conference*, pp. 171 –179, 16- 20 June 2003.

[2] Libert F., Soulard J., "Design Study of a Direct-Driven Surface Mounted Permanent Magnet Motor for Low Speed Application", *Symposium on Advanced Electromechanical Motion Systems Electromotion* 2003, vol. 1 pp. 252-257, 26-28 November 2003, Marrakesh, Morocco.

[3] Magnussen F., Sadarangani C., "Winding Factors and Joule Losses of Permanent Magnet Machines with Concentrated Windings", *Electric Machines and Drives Conference (IEMDC'03)*, vol. 1, pp. 333-339, June 2003.

[4] Cros J., Viarouge P., "Synthesis of High Performance PM Motors with Concentrated Windings", *IEEE Transactions on Energy Conversion*, vol. 17 Issue: 2, pp. 248 –253, June 2002.

[5] Ishak D., Zhu Z.Q., Howe D., "Comparative Study of Permanent Magnet Brushless Motors with All Teeth and Alternative Teeth Windings", *IEE International conference on Power Electronics and Electrical Machines (PEMD)*, March-April 2004, Edinburgh, United Kingdom.

[6] Ivanov-Smolenski A., "Electrical Machines", Moscow: Mir Russia, 1982.

[7] Libert F., Soulard J., "Design Study of Different Direct-Driven Permanent-Magnet Motors for a Low Speed Application", Nordic Workshop on Power and Industrial Electronics (NORpie), Trondheim, Norway, June 2004.

[8] Maliti K.C., Sadarangani C., "Modelling Magnetic Noise in Induction Machines", *International Conference on Electrical Machines*, pp. 406-410, September 1997, Cambridge, U.K.